Efficient temporal shaping of electron distributions for high-brightness photoemission electron guns

Ivan V. Bazarov,* Dimitre G. Ouzounov, Bruce M. Dunham, Sergey A. Belomestnykh, Yulin Li, Xianghong Liu, Robert E. Meller, John Sikora, and Charles K. Sinclair

Laboratory for Elementary Particle Physics, Cornell University, Ithaca, New York 14853, USA

Frank W. Wise

Department of Applied and Engineering Physics, Cornell University, Ithaca, New York 14853, USA

Tsukasa Miyajima

Photon Factory, KEK, Tsukuba, Japan

To achieve the lowest emittance electron bunches from photoemission electron guns, it is essential to limit the uncorrelated emittance growth due to space charge forces acting on the bunch in the vicinity of the photocathode through appropriate temporal shaping of the optical pulses illuminating the photocathode. We present measurements of the temporal profile of electron bunches from a bulk crystal GaAs photocathode illuminated with 520 nm wavelength pulses from a frequency-doubled Yb-fiber laser. A transverse deflecting rf cavity was used to make these measurements. The measured laser pulse temporal profile and the corresponding electron beam temporal profile have about 30 ps FWHM duration, with rise and fall times of a few ps. GaAs illuminated by 520 nm optical pulses is a prompt emitter within our measurement uncertainty of ~1 ps rms. Combined with the low thermal emittance of negative electron affinity photocathodes, GaAs is a very suitable photocathode for high-brightness photoinjectors. We also report measurements of the photoemission response time for GaAsP, which show a strong dependence on the quantum efficiency of the photocathode.

I. INTRODUCTION

Novel accelerator applications based on the energy recovery linac (ERL) concept [1–4] require an electron source delivering both high average current and low beam emittance. Photoemission electron guns with high quantum efficiency (QE) cathode materials provide a natural route to meeting the requirements of an ERL injector. The negative electron affinity (NEA) class of photocathodes is of particular interest given their low thermal emittance [5] and high QE. Assuming the injector optics is tuned to achieve optimal emittance compensation [6], it should be possible [7] to achieve an emittance approaching the thermal emittance of the photocathode. For illumination by a short duration laser pulse with a top-hat transverse profile, this is given by

$$\epsilon_{n,x} = \sqrt{\frac{q}{4\pi\epsilon_0 E_{\text{cath}}} \frac{k_B T_\perp}{m_e c^2}}, \qquad (1)$$

where q is the bunch charge, $k_B T_\perp$ is the (transverse) cathode thermal energy, E_{cath} is the electric field at the cathode, and ϵ_0 and $m_e c^2$ are the vacuum permittivity and the electron rest energy, respectively. Equation (1) represents the lowest possible normalized emittance in the case of space charge limited extraction from the cathode. To

produce bunches with an emittance approaching the thermal emittance, however, it is essential to achieve a very high degree of emittance compensation, requiring in turn that the uncorrelated emittance growth associated with space charge forces be minimized. Minimization of this uncorrelated emittance growth requires a 3D shaping of the initial electron distribution, by shaping the illuminating laser pulse spatially and temporally [7–14]. The optimal 3D shape depends on the operating parameters such as the charge per bunch and the accelerating gradient at the cathode. Normally the transverse and longitudinal pulse profiles cannot be optimized independently. Efficient temporal shaping requires a prompt photoemitter (< 1 ps response time for accelerators operating at ~1 GHz rf frequency), and operation at high average current strongly favors a laser shaping technique with minimal insertion losses, to minimize the required laser average power. In this paper we present measurements that demonstrate an efficient process for temporal pulse shaping [15] of the electron bunch and a fast ($\leq$ ps) response time of NEA GaAs photocathodes.

The paper is organized as follows. Section II summarizes the experimental setup used to carry out the measurements of the electron temporal profiles from a high voltage DC photoemission electron gun. Section III presents experimental comparisons of temporal profile measurements of both the electron and laser pulses. Section IV presents the measured response time of two photocathode types,
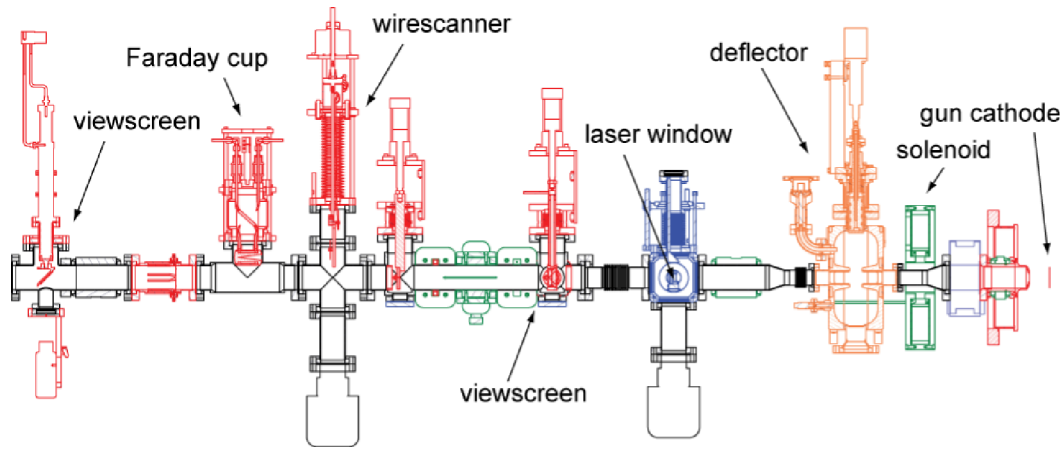
---

*ib38@cornell.edu

FIG. 1. (Color) Beam line used for temporal profile measurements. Beam direction is to the left.

GaAs and GaAsP, when excited by an unshaped laser pulse of 1.0 ps rms duration. We conclude with a discussion and summary.

II. EXPERIMENTAL SETUP

The beam line section used for the measurements is shown in Fig. 1. The high voltage DC gun [16] is equipped with a load-lock system to allow photocathode activation external to the gun, and relatively rapid exchange of photocathodes between the gun and activation chambers. A low ripple ($< 10^{-4}$ rms) 120 kV DC power supply provided the gun voltage for these measurements. The electron beam was focused with a solenoid magnet to a spot size of 0.2 mm rms on a BeO viewscreen located downstream of a vertical deflection rf cavity [17]. The electron beam bunches transited this cavity at the zero crossing of the rf field. To make the space charge effects inconsequential for these measurements, we operated with a typical average current of about 1 nA with a 50 MHz bunch repetition rate, corresponding to ~ 125 electrons/bunch. It was established both by space charge calculations and by varying the laser intensity and thus the average beam current that there was no bunch lengthening due to space charge in these measurements.

The laser system used in these studies has been described elsewhere [18]. The system consists of a soliton Yb-fiber laser oscillator, a single-mode fiber preamplifier, and a double-clad large mode area fiber amplifier (Fig. 2). The system provides 5 W average infrared power delivered in 3 ps FWHM pulses at 50 MHz. These pulses are efficiently frequency-doubled to produce 2.3 ps FWHM (1.0 ps rms) pulses at 520 nm using a lithium triborate crystal (marked as SHG LBO in Fig. 2; SHG stands for second harmonic generation). Temporal shaping of the laser pulses is performed by "pulse stacking" using several birefringent crystals of different lengths [15]. The laser profile after shaping is measured with a cross correlator using the unshaped primary pulse as a reference. Mea-

surement of both orthogonal polarizations is necessary to reconstruct the temporal laser profile. Finally, the setup is equipped with a delay stage used to calibrate the timing scale of the cross correlator and the deflecting cavity (Fig. 3).

Given the small loaded Q and consequent large bandwidth of the deflection cavity, we chose to synchronize the rf to the laser. An avalanche photodiode illuminated by a fraction of the 50 MHz train of laser pulses generated a 50 MHz electrical pulse train. This was passed through a 1.3 GHz bandpass filter and amplified to drive the rf cavity. The synchronization between the rf and the laser was measured directly using a sampling scope (Agilent 86100C) to be 1.2 ± 0.2 ps rms.

As in Ref. [5], two cathodes have been used in these studies: GaAs and GaAsP. GaAs wafers [surface (100) tilted 2° off toward the $\langle 110 \rangle$ direction] with Zn doping
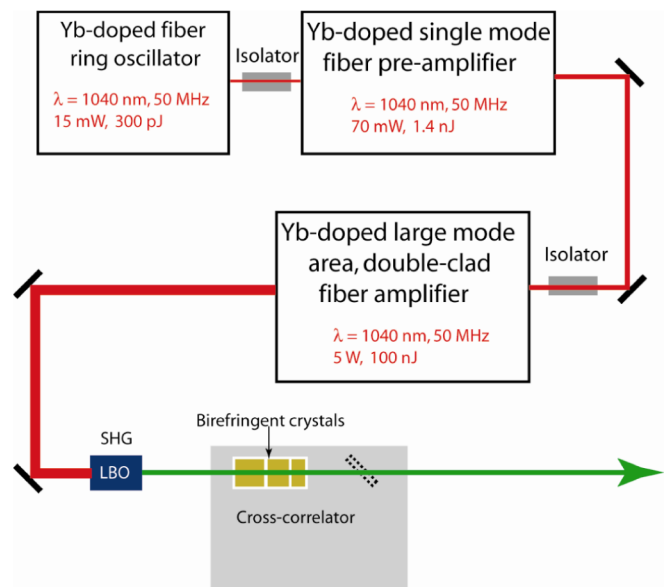

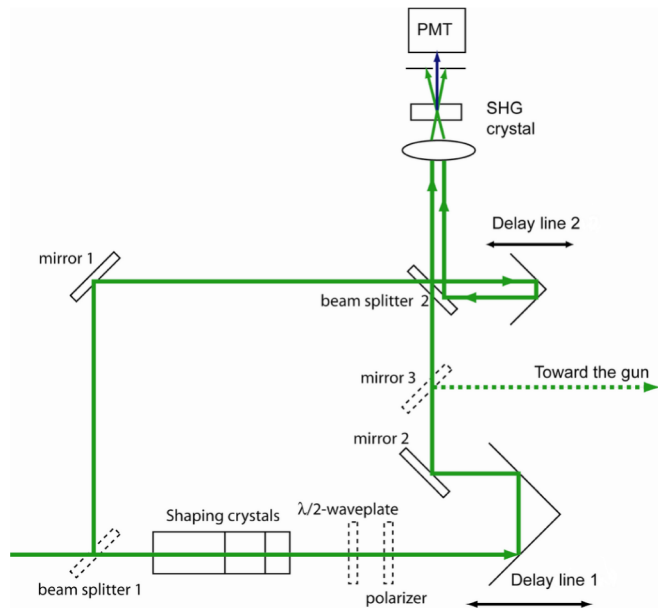FIG. 2. (Color) Schematic of the laser system.

FIG. 3. (Color) Cross-correlator setup. Beam splitter 1 (BS1) and mirror 3 (M3) are on flipper mounts. When cross correlation is measured, BS1 is flipped up, M3 is flipped down, and the polarizer and the half-waveplate are inserted. When the laser beam drives the gun, BS1 is down, M3 is up, the wave plate and the polarizer are removed. Delay line 1 is used to set the time scale of the deflector cavity and the cross correlator.

between 6.3×10^{18} and 1.9×10^{19} cm^{-3} were activated in the cathode activation chamber of the load-lock system. A yo-yo activation with cesium and nitrogen trifluoride gave typical initial quantum efficiencies of 10% at 532 nm. GaAsP photocathodes were activated in a similar fashion. The GaAsP was grown by molecular-beam epitaxy on GaAs substrates to a thickness of 2 μm. The phosphorus concentration was ~45% with a *p*-doping level of 2–4 $\times$ 10^{18} cm^{-3}. A 2 μm transition layer with graded phosphorus concentration separated the GaAs substrate and the GaAsP active layer to minimize the strain resulting from the lattice mismatch between GaAs and GaAsP.

III. TEMPORAL PULSE SHAPING

The use of birefringent crystals for pulse shaping has been proposed [19] and demonstrated elsewhere [15]. The crystals used in this work were *a*-cut YVO$_4$. The lengths of the crystals, 13.60, 6.86, 3.44, and 1.71 mm, determine the separation between the individual output pulses, given by the 1.05 ps/mm group velocity delay difference for propagation along the fast and slow axes of this crystal material. All crystal surfaces were antireflection coated with a specified insertion loss of <0.2% per surface. Since the crystals have their optical axis parallel to the front surfaces, there is no spatial walk-off between ordinary and extraordinary beams at perfect normal incidence. During alignment, the back reflection from the front surface is used to ensure that

the incidence is close normal. A very small spatial walk-off is possible due to the angle tolerance of the crystal cut, which is specified at $\pm 0.5°$ for optical axis orientation. The walk-off is estimated to be no more than about 10 μm per 1 cm of propagation in the crystals, which is negligible compared to the laser beam diameter. Even in this case, the beams remain parallel after the crystals. The laser pulses were transported some 15 m to the gun location.

The angles between fast and slow axes of the first crystal and the linear polarization of the incident laser light is 45°. Subsequent crystals are also oriented with fast and slow axes at 45° to the incident optical polarizations, so that a temporally distinct pulse is split into two pulses with orthogonal polarizations traveling at different group velocities in each crystal. The resulting temporal profile is a modulated flattop with the rise and fall times of the original unshaped pulse (see Fig. 4). We point out that this technique can be used to construct other pulse shapes of interest for low emittance beam production, such as temporal profiles with a depression in the middle [7], or an approximation to an elliptical profile [10], through simple rotations of the crystals with respect to each other, e.g., see Fig. 4.

Figures 5–7 show experimental measurements of pulse shaping step by step, using a three crystal array. The top curves show optical cross-correlation measurements of the optical pulse, while the bottom curves show the electron beam temporal profiles as determined by the deflecting cavity measurements. The photocathode material used in these measurements is GaAs.

Any scale error of the time axis is estimated to be no greater than 5%. For the intensity measurement uncer-
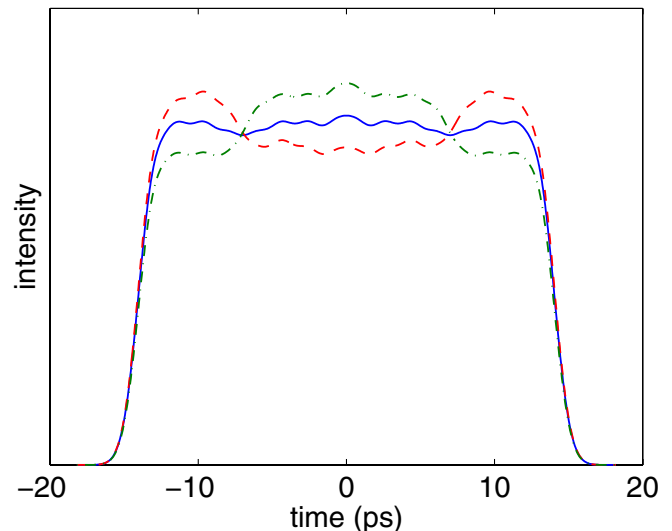

FIG. 4. (Color) Calculated temporal shape for given crystal lengths and materials. Orientations of the optical axis of each of the four crystals with respect to the incident laser polarization direction (0°) are as following: 45°, 0°, 45°, −0.7° (solid); 45°, 2°, 47.4°, 1.5° (dashed); 45°, −2.4°, 42.6°, −2.9° (dot-dashed line).
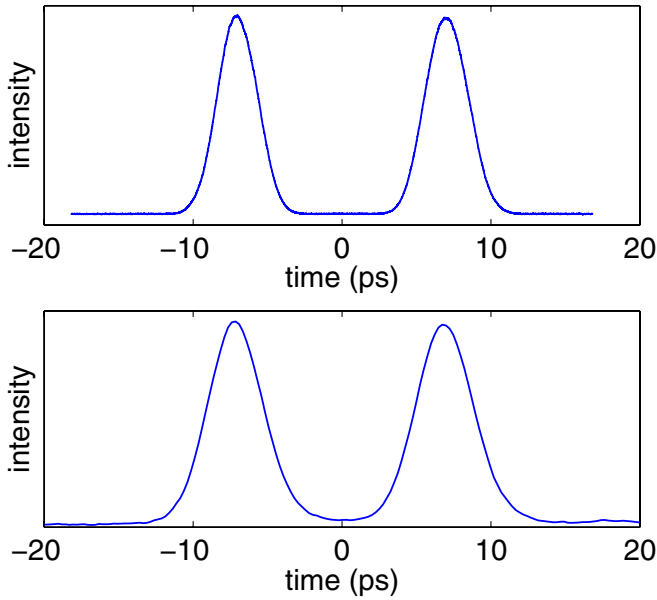
FIG. 5. (Color) Laser pulse (top) and electron bunch (bottom) temporal profile measurement after a single (longest) shaping crystal.

tainty, we place a conservative upper estimate of 10% due to possible error sources such as nonuniformity of the BeO viewscreen. In addition, the data for the electron bunch temporal profile from the viewscreen represents an average over 3 frames. Each image has been subject to 3×3 median filtering to minimize the effect of "zingers" (random extreme pixel values due to scattered x rays). No other filtering has been done.
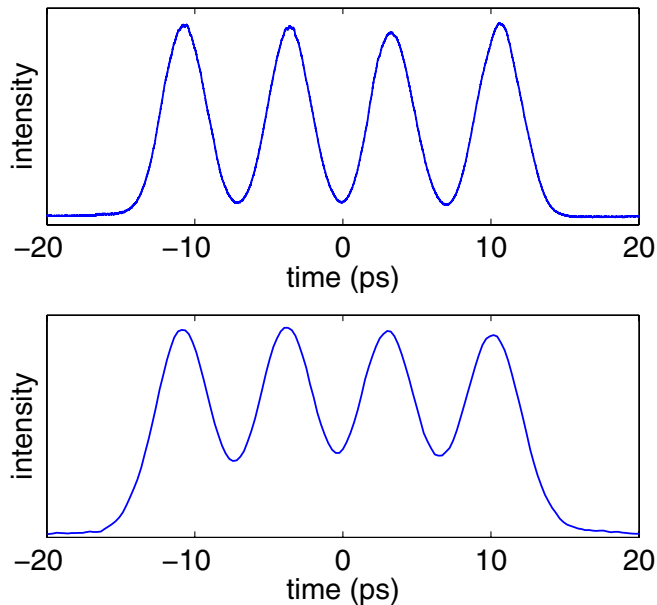

FIG. 6. (Color) Laser pulse (top) and electron bunch (bottom) temporal profile measurement after two shaping crystals.
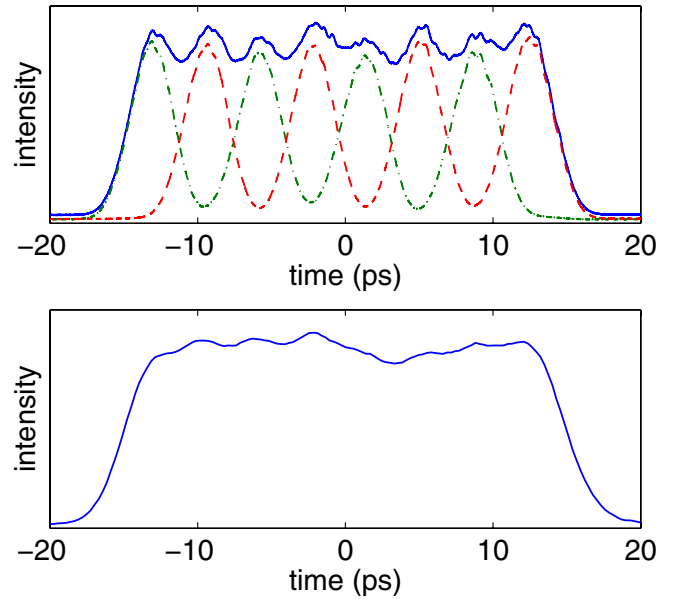

FIG. 7. (Color) Laser pulse (top) and electron bunch (bottom) temporal profile measurement after three shaping crystals. Laser cross correlation shows the intensity of the two orthogonal polarizations (dashed and dot-dashed) and their sum (solid line). The ripple of the flattop region of the distributions corresponding to these plots is 6.1% rms for the laser and 4.2% rms for the electron beams.

The effect of the 4th crystal (not shown) cannot be resolved using our rf deflection system, which has an estimated resolution of 1.5 ps rms in addition to the 1.0 ps rms laser pulse duration. It can be seen from these figures that a very good agreement exists between the measured temporal profiles of the laser and electron beams, and that photoemission from GaAs at this wavelength is sufficiently prompt to faithfully reproduce the temporal shape of the laser pulse.

IV. PHOTOCATHODE RESPONSE TIME

Figure 8 shows the electron pulses from a GaAs photocathode (5% and 10% QE) illuminated with 1 ps rms duration laser pulses. A Gaussian fit to the QE = 5% data yields an rms width of the electron pulse of 1.8 ps. The dashed curve shows the contribution to the timing resolution from the finite vertical size of the electron beam on the viewscreen (obtained with the rf deflector off). The width of the measured pulse can be fully accounted for by three contributions: the rf to laser synchronization jitter (1.2 ps rms), the laser pulse duration (1.0 ps rms), and the finite spot size of the electron beam (equivalent to 0.9 ps rms).

Figure 9 shows the temporal response of GaAsP photocathodes with different values of QE. A strong dependence of the response time on QE is seen. A noticeable tail begins to form when QE ≥ 1%. A similar, although much smaller,
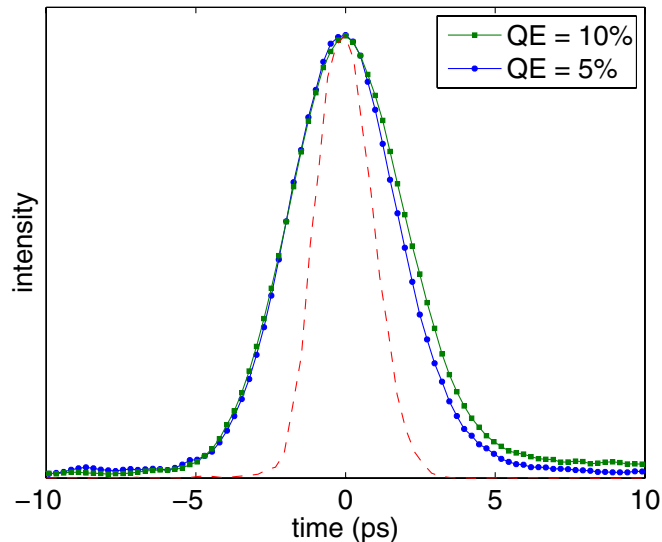
FIG. 8. (Color) Temporal response obtained from GaAs (QE = 5, 10%) excited by 1 ps rms 520 nm laser pulse. The dashed line shows the profile obtained when the deflecting cavity is not powered. Gaussian fits provide 1.8 ps (solid, QE = 5%) and 0.9 ps (dashed) standard deviation. Refer to text for the information on the measurement resolution.
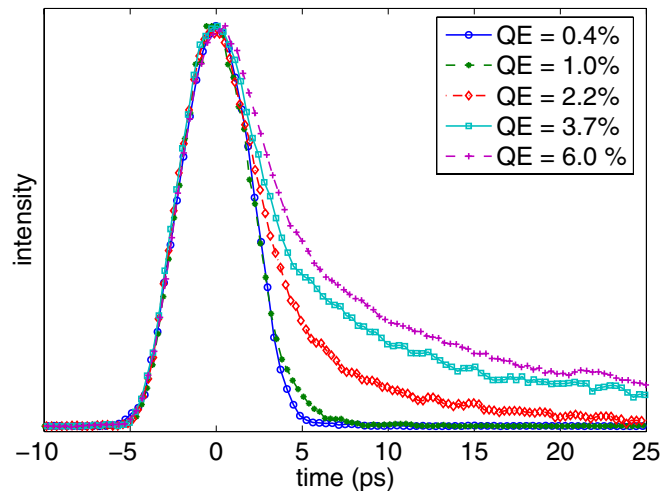

FIG. 9. (Color) Temporal response obtained from GaAsP excited by 1 ps rms 520 nm laser pulse for different QE values.

dependence of the response time on QE was observed for GaAs, see Fig. 8. For GaAs, a noticeable tail begins to form when QE $\geq$ 6%, whereas no tail could be observed in our measurements for lower QE values.

V. DISCUSSION AND SUMMARY

We have demonstrated a very efficient method of producing temporally shaped electron bunches from NEA GaAs photocathodes using laser pulse stacking in a series of birefringent crystals. In addition, we have measured the temporal response time at 520 nm of both GaAs and

GaAsP photocathodes. The temporal response of GaAsP photocathodes is within the resolution of our experimental setup for QE < 1%, of GaAs for QE < 6%. These results are consistent with measurements using an indirect method based on computations of the space charge bunch lengthening that we reported earlier for these photocathodes [5]. As explained in Ref. [5], the photoemission response time of GaAs at 520 nm is much faster than for illumination with near band-gap wavelengths, due to the dependence of optical absorption in the semiconductor on wavelength. This is fully consistent with the α^{-2} scaling of the temporal response time predicted by diffusion models, where α is the optical absorption constant [20,21].

In addition, we have found that the surface condition, as characterized by QE, has a dramatic effect on the temporal response of GaAsP photocathodes, and to a much lesser degree for GaAs photocathodes. The exact theoretical model behind this effect is not clear to us at the moment. We note, however, that the larger thermal emittance of GaAsP [5] as well as the photoemitted electron energy spectra measurements using a parallel-plate geometry [22] clearly indicate that the emission occurs from both the Γ and X conduction band minima. Emission from the X minimum is indirect and involves additional momentum exchange as opposed to the emission from the Γ-minimum, and could be responsible for the longer temporal response time as well as the larger transverse thermal emittance. Emission from the X minimum may be suppressed by decreasing the phosphorous content of the GaAsP alloy, possibly giving a smaller transverse emittance and a faster temporal response.

[1] M. Tigner, Nuovo Cimento **37**, 1228 (1965).
[2] S. Benson *et al.*, in *Proceedings of the 2007 Particle Accelerator Conference* (IEEE, Albuquerque, NM, 2007), pp. 79–81.
[3] S. M. Gruner and M. Tigner, CHESS Technical Memo 02-003, Jefferson Laboratory Report No. JLABACT-01-04, 2001.
[4] I. Ben-Zvi, in *Proceedings of the 2006 European Particle Accelerator Conference* (EPS-AG and CERN, Edinburgh, Scotland, 2006), pp. 940–944.
[5] I. V. Bazarov, B. M. Dunham, Y. Li, X. Liu, D. G. Ouzounov, C. K. Sinclair, F. Hannon, and T. Miyajima, J. Appl. Phys. **103**, 054901 (2008).
[6] B. E. Carlsten, Nucl. Instrum. Methods Phys. Res., Sect. A **285**, 313 (1989).
[7] I. V. Bazarov and C. K. Sinclair, Phys. Rev. ST Accel. Beams **8**, 034202 (2005).

[8] H. Tomizawa, T. Asaka, H. Dewa, H. Hanaki, T. Kobayashi, A. Mizuno, S. Suzuki, T. Taniuchi, and K. Yanagida, in *Proceedings of the 8th European Particle Accelerator Conference, Paris, 2002* (EPS-GA and CERN, Geneva, 2002), p. 1819.

[9] J. Yang *et al.*, J. Appl. Phys. **92**, 1608 (2002).

[10] C. Limborg-Deprey and P. R. Bolton, Nucl. Instrum. Methods Phys. Res., Sect. A **557**, 106 (2006).

[11] O. J. Luiten, S. B. van der Geer, M. J. de Loos, F. B. Kiewiet, and M. J. van der Wiel, Phys. Rev. Lett. **93**, 094802 (2004).

[12] Y. Li and J. W. Lewellen, Phys. Rev. Lett. **100**, 074801 (2008).

[13] R. Akre *et al.*, Phys. Rev. ST Accel. Beams **11**, 030703 (2008).

[14] A. Cianchi *et al.*, Phys. Rev. ST Accel. Beams **11**, 032801 (2008).

[15] S. Zhou, D. G. Ouzounov, H. Li, I. V. Bazarov, B. M. Dunham, C. K. Sinclair, and F. W. Wise, Appl. Opt. **46**, 8488 (2007).

[16] B. M. Dunham, C. K. Sinclair, I. V. Bazarov, Y. Li, X. Liu, and K. W. Smolenski, in Proceedings of the 2007 Particle Accelerator Conference, Ref. [2], p. 1224.

[17] S. Belomestnykh, V. Shemelin, K. Smolenski, and V. Veshcherevich, in Proceedings of the 2007 Particle Accelerator Conference, Ref. [2], p. 2331.

[18] D. G. Ouzounov, I. V. Bazarov, B. M. Dunham, C. K. Sinclair, S. Zhou, and F. Wise, in Proceedings of the 2007 Particle Accelerator Conference, Ref. [2], p. 530.

[19] H. E. Bates, R. R. Alfano, and N. Schiller, Appl. Opt. **18**, 947 (1979).

[20] P. Hartmann, J. Bermuth, D. v. Harrach, J. Hoffmann, S. Kbis, E. Reichert, K. Aulenbacher, J. Schuler, and M. Steigerwald, J. Appl. Phys. **86**, 2245 (1999).

[21] K. Aulenbacher, J. Schuler, D. v. Harrach, E. Reichert, and J. Rthgen, J. Appl. Phys. **92**, 7536 (2002).

[22] A. W. Baum, W. E. Spicer, R. F. Pease, K. A. Kostello, and V. W. Aebi, in *SPIE Proceedings* (SPIE, Bellingham, WA, 1995), Vol. 2550, p. 189.